

Airborne Weather Radar Concept for Measuring Water Surface Backscattering Signature and Sea Wind at Circular Flight

Koncept meteo radara u zrakoplovu za mjerenje brzine vjetra na moru s pomoću refleksije s morske površine u kružnom letu

Alexey Nekrasov

Saint Petersburg Electrotechnical University, Saint Petersburg, Russia
Southern Federal University, Taganrog, Russia
Hamburg University of Technology, Hamburg, Germany
e-mail: alexei-nekrassov@mail.ru

Vladimir Veremyev

Saint Petersburg Electrotechnical University
Saint Petersburg, Russia
e-mail: ver_vi@mail.ru

DOI 10.17818/NM/2016/4.5

UDK 551.556

Original scientific paper / Izvorni znanstveni rad
Paper accepted / Rukopis primljen: 25. 4. 2016.

Summary

A concept for measuring water surface backscattering signature and wind over sea using airborne weather radar is discussed. The radar operates in the ground-mapping mode as a scatterometer, in addition to its meteorological and navigation application. An aircraft circular flight is used under such measurement. Recommendations to perform measurement of the water surface backscattering signature along with a sea wind retrieval algorithm are proposed. A simulation study of wind vector estimation is performed. The results obtained show that airborne weather radar can provide reasonable sea wind vector retrieval accuracy.

KEY WORDS

sea wind
water surface backscattering
airborne weather radar
algorithm

Sažetak

U radu se govori o konceptu mjerenja brzine vjetra na moru s pomoću refleksije s morske površine upotrebom meteoradara u zrakoplovu. Osim što ima funkciju u meteorologiji i navigaciji, radar služi i kao mjerač raspršenja. Mjerenje je obavljeno u zrakoplovu u kružnom letu. U radu se daju preporuke za mjerenje refleksije s morske površine i algoritma brzine vjetra na moru. Izvršena je simulacija procjene vektora vjetra. Dobiveni rezultati ukazuju da meteoradar u zrakoplovu može dati prilično precizne podatke o vektoru vjetra na moru.

KLJUČNE RIJEČI

vjetar na moru
refleksija s morske površine
meteoradar u zrakoplovu
algoritam

1. INTRODUCTION / Uvod

Microwave backscattering signatures of water surface are investigated by many researchers actively [1-13]. The typical method for describing sea clutter is in the form of the normalized radar cross section (NRCS), the statistical distribution of the NRCS, the amplitude correlation and the spectral shape of the Doppler returns.

To explain adequately the microwave scattering signature of water surface and to apply its features to remote sensing series of experiments are required: experimental verification of combined frequency, azimuth and incidence angles and wind speed variations of the NRCS [5]. For such a study, a scatterometer, i.e. radar designed for measuring the surface scatter characteristics, is used.

Research on microwave backscatter by water surface has shown that the use of a scatterometer also allows an estimation of near-surface wind speed and direction because the NRCS of sea surface depends on wind speeds and directions. Based on experimental data and scattering theory, a significant number

of empirical and theoretical backscatter models and algorithms for estimation of a near-surface wind vector from satellite and airplane has been developed [14].

To study a microwave backscattering signature of water surface from aircraft, an airborne scatterometer is used. The measurements are typically performed at either a circular track flight using fixed fan-beam antenna or a rectilinear track flight using rotating antenna [5, 6, 8]. Unfortunately, a microwave narrow-beam antenna has considerable size at Ku-, X- and C-bands that makes its placing on aircraft difficult. Therefore, a better solution needs to be found.

At least two methods can be proposed. The first method is to apply the airborne scatterometers with wide-beam antennas as it can lead to reduction in the antenna size. The second method is to use the modified conventional navigation instruments of aircraft in a scatterometer mode that seems more preferable.

From that point of view, a promising navigation instrument is airborne weather radar (AWR). In this connection, a possibility

to measure the sea surface backscattering signature and to retrieve the wind speed and direction over water by the AWR in the scatterometer mode at an aircraft circular flight, in addition to its standard navigation application, is discussed in this paper.

2. GENERAL DESCRIPTION OF AIRBORNE WEATHER RADAR / Opis meteoradara u zrakoplovu

AWR is radar equipment mounted on aircraft for weather observation and avoidance, aircraft position finding relative to landmarks, and drift angle measuring [15]. The AWR is required equipment for any civil aircraft. All military transport aircraft are usually equipped with weather radars too. Due to specificity of airborne application, designers of avionics systems always try to use the most efficient methods and reliable engineering solutions, which provide safety and regularity of flying in harsh environment [16, 17].

Development of AWR is mainly associated with growing functionalities on detection of different dangerous weather phenomena. The radar observations involved in a weather mode are magnitude detection of reflections from clouds and precipitation, and Doppler measurements of the motion of particles within weather formations. Magnitude detection allows determination of particle type (rain, snow, hail, etc.) and precipitation rate. Doppler measurements can be made to yield estimates of turbulence intensity and wind speed. Reliable determination of the presence and severity of the phenomenon known as wind shear is an important area of study too [18].

The second important assignment of the AWR is providing a pilot with navigation information using earth surface mapping. In this case, a possibility to extract some navigation information that allows determining aircraft position with respect to a geographic map is very important for air navigation. Landmark's coordinates relative to the aircraft measured by the AWR allow setting a flight computer for a more exact and more efficient en-route flying, cargo delivery, and cargo throw down to the given point. These improve tactical possibilities of transport aircraft, airplanes of search-and-rescue service, and local airways [16].

Other specific function of the AWR is interaction with ground-based responder beacons. New functions of the AWR are detection and visualization of runways at approach landing as well as visualization of taxiways and obstacles on the taxiway at taxiing.

Certainly, not all of the mentioned functions are implemented in a particular airborne radar system. Nevertheless, the AWR always is a multifunctional system that provides earth surface surveillance and weather observation. Usually, weather radar should at least enable to detect clouds and precipitation, select zones of meteorological danger, and show radar image of surface in the map mode.

AWRs or multimode radars with a weather mode are usually nose mounted. Most AWRs operate in either X- or C-band [18]. The λ^{-4} dependence of weather formations on carrier wavelength λ favours X-band radar for their detecting. At the same time, the X-band provides the performance of the long-range weather mode better than Ku-band. The AWR antenna, in the ground-mapping mode, has a large cosecant-squared elevation beam where horizontal dimension is narrow (2° to 6°) while the other is relatively broad (10° to 30°), and it sweeps in an azimuth sector

(up to $\pm 100^\circ$) [18], [19]. The scan plane is horizontal because the antenna is stabilized (roll-and-pitch-stabilized). These features allow the presumption that AWR operating in the ground-mapping mode can be used as a scatterometer for measuring the water surface backscattering signature and near-surface wind over water.

3. MEASUREMENT OF BACKSCATTERING SIGNATURE / Mjerenje refleksije

Let an aircraft equipped with an AWR make a horizontal rectilinear flight with the speed V at some altitude H above the mean sea surface, the AWR operate in the ground-mapping mode as a scatterometer, the radar antenna have different beam width in the vertical $\theta_{a,v}$ and horizontal $\theta_{a,h}$ planes ($\theta_{a,v} > \theta_{a,h}$), and scan periodically through an azimuth in a sector as shown in Fig. 1. Also let a delay selection be used to provide necessary resolution in the vertical plane.

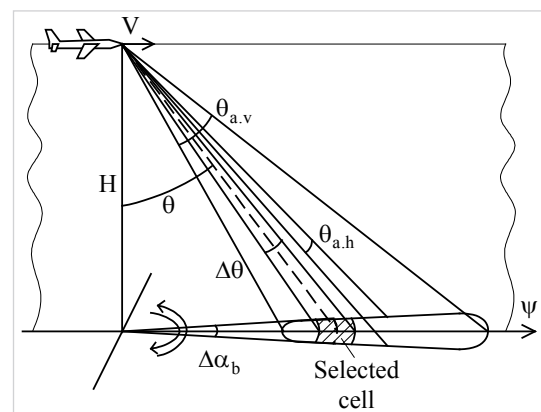


Figure 1 Scanning beam and selected cell geometry
Slika 1. Skeniranje zraka i geometrija odabrane ćelije

The scanning beam allows selecting a power backscattered by the underlying surface for given incidence angle θ from various directions in an azimuth sector relative to the aircraft course ψ . Angular selection (narrow horizontal beam width) in the horizontal plane along with the delay selection provides angular resolutions in the azimuthal and vertical planes, $\Delta\alpha_b$ and $\Delta\theta$ respectively. A current NRCS value obtained from the selected cell is $\sigma^\circ(\theta, \psi + \psi_b)$, where ψ_b is the current azimuth direction of the beam relative to the aircraft current course (right position is positive).

If the azimuth direction of the beam relative to the aircraft current course is fixed, the azimuth NRCS curve can be obtained using the circular track flight. As the scan plane is horizontal because the antenna is stabilized, the aircraft roll should not exceed the maximum one allowed for ensuring the antenna stabilization and consequently the incidence angle constancy.

Let a horizontal circular flight with the speed V and the left roll at some altitude H above the mean sea surface be completed (Fig. 2). The fixed beam should be pointed to the outer side of the aircraft turn to observe a greater area of the water surface and to obtain a greater number of independent NRCS samples. From that point of view, the best beam position is when the azimuth direction of the beam is perpendicular to the aircraft current course.

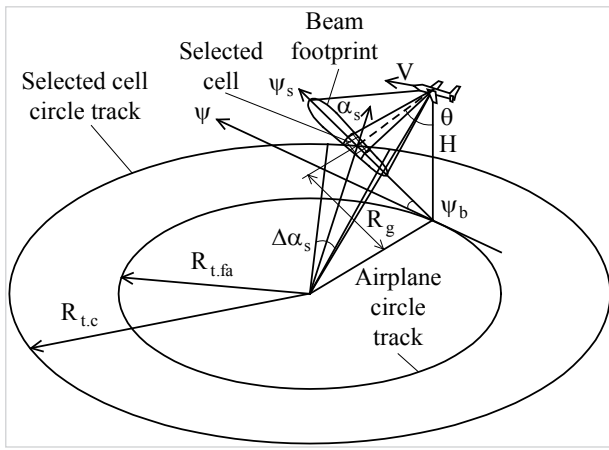


Figure 2 Measuring geometry: $R_{t,fa}$ is the radius of aircraft turn, R_g is the ground range, $R_{t,c}$ is the radius of turn of the selected cell middle point

Slika 2. Geometrija mjerenja: $R_{t,fa}$ je radijus okreta zrakoplova, R_g je udaljenost od tla, $R_{t,c}$ je radijus okreta središnje točke odabrane ćelije

The azimuth size of a sector observed is 5° or 10° , respectively. A middle azimuth of the sector is the azimuth of the sector observed. The azimuth size of a sector relative to the centre point of circle of the airplane track is $\Delta\alpha_s$, and the middle azimuth of a sector is α_s . The NRCS samples obtained from the sector and averaged over all measurement values in that sector give the NRCS value $\sigma^\circ(U, \theta, \psi_s)$ corresponding to the real observation azimuth angle of the sector ψ_s that is

$$\psi_s = \psi_{\psi_s} + \psi_b \pm 360^\circ, \quad (1)$$

where ψ_{ψ_s} is the airplane course corresponding to the real observation azimuth angle of the sector.

The 360-degree azimuth space can be divided into 72 or 36 sectors under the circle NRCS measurement. Thus, to obtain an azimuth NRCS curve of water surface in the range of moderate to high incidence angles under aircraft circular flight by the AWR operating in the ground-mapping mode as a scatterometer, the measurement should be started when a stable flight at the given altitude, speed of flight, roll and pitch has been established. Measurement should be finished when the azimuth of the measurement beginning is reached. To obtain a greater number of NRCS samples for each sector observed several consecutive full circular turns for 360° may be done.

4. WIND VECTOR RETRIEVAL / Izračun vektora vjetrova

The wind blowing over sea modifies surface backscatter properties. These depend on wind speed and direction. Wind speed U can be measured by a scatterometer because a stronger wind produces a larger NRCS $\sigma^\circ(U, \theta, \alpha)$ at a medium incidence angle θ , and a smaller NRCS at the small (near nadir) incidence angle. Wind direction can also be inferred because NRCS varies as a function of azimuth illumination angle α relative to up-wind direction [7].

To retrieve the wind vector from NRCS measurements, a relationship between the NRCS and near-surface wind, called "geophysical model function," must be known. Scatterometer experiments have shown that the NRCS model function for medium incidence angles at appropriate transmit and received

polarization (vertical or horizontal) is one of the widely used form [20]

$$\sigma^\circ(U, \theta, \alpha) = A(U, \theta) + B(U, \theta) \cos \alpha + C(U, \theta) \cos(2\alpha), \quad (2)$$

where $A(U, \theta)$, $B(U, \theta)$ and $C(U, \theta)$ are the Fourier terms that depend on sea surface wind speed and incidence angle, $A(U, \theta) = a_0(\theta)U^{\gamma_0(\theta)}$, $B(U, \theta) = a_1(\theta)U^{\gamma_1(\theta)}$ and $C(U, \theta) = a_2(\theta)U^{\gamma_2(\theta)}$; $a_0(\theta)$, $a_1(\theta)$, $a_2(\theta)$, $\gamma_0(\theta)$, $\gamma_1(\theta)$ and $\gamma_2(\theta)$ are the coefficients dependent on the incidence angle, radar wave length, and polarization.

As the measured NRCS data set is also a function of the wind speed, each NRCS value $\sigma^\circ(\theta, \psi_{s,i})$ obtained for a sector i is considered now as $\sigma^\circ(U, \theta, \psi_{s,i})$.

Let the angle between the up-wind direction and the first NRCS azimuth $\psi_{s,1}$ be α , the sector width be $\Delta\alpha_s$, and the measured NRCSs $\sigma^\circ(U, \theta, \psi_{s,1})$, $\sigma^\circ(U, \theta, \psi_{s,2})$, ..., and $\sigma^\circ(U, \theta, \psi_{s,N})$ be as $\sigma^\circ(U, \theta, \alpha)$, $\sigma^\circ(U, \theta, \alpha - \Delta\alpha_s)$, ..., and $\sigma^\circ(U, \theta, \alpha - (N-1)\Delta\alpha_s)$, respectively, where $i = \overline{1, N}$, N is the number of sectors composing the measured 360° azimuth NRCS curve, $N = 360^\circ / \Delta\alpha_s$. Then, in a general case, to find the wind speed and up-wind direction from the azimuth NRCS data set obtained the following system of N equations should be solved

$$\left\{ \begin{array}{l} \sigma^\circ(U, \theta, \alpha) = A(U, \theta) + B(U, \theta) \cos \alpha \\ \quad + C(U, \theta) \cos(2\alpha), \\ \sigma^\circ(U, \theta, \alpha - \Delta\alpha_s) = A(U, \theta) \\ \quad + B(U, \theta) \cos(\alpha - \Delta\alpha_s) \\ \quad + C(U, \theta) \cos(2(\alpha - \Delta\alpha_s)), \\ \dots\dots\dots \\ \sigma^\circ(U, \theta, \alpha - (N-2)\Delta\alpha_s) = A(U, \theta) \\ \quad + B(U, \theta) \cos(\alpha - (N-2)\Delta\alpha_s) \\ \quad + C(U, \theta) \cos(2(\alpha - (N-2)\Delta\alpha_s)), \\ \sigma^\circ(U, \theta, \alpha - (N-1)\Delta\alpha_s) = A(U, \theta) \\ \quad + B(U, \theta) \cos(\alpha - (N-1)\Delta\alpha_s) \\ \quad + C(U, \theta) \cos(2(\alpha - (N-1)\Delta\alpha_s)), \end{array} \right. \quad (3)$$

and the navigation wind direction can be found as following

$$\psi_w = \psi_{s,1} - \alpha \pm 180^\circ. \quad (4)$$

To investigate capability of the proposed wind algorithm, a simulation of the wind vector retrieval based on a Wismann's geophysical model function [6] of the form (2) for the incidence angle of 45° was performed. The "measured" azimuth NRCS values were generated using Rayleigh Power (Exponential) distribution.

Fig. 3 shows "measured" NRCS after averaging of 44 samples in a one-degree azimuth sector at the "true" wind speed of 10 m/s (dot trace), and Fig. 4 demonstrates "measured" NRCS after averaging of 220 samples in a five-degree azimuth sector at the same wind speed (dot trace). Solid traces in these figures show the azimuth NRCS curves by model (1).

Using system of equations (3), the "measured" wind speed is 9.95 m/s for the "true" wind speed of 10 m/s, and the "measured" up-wind direction is 355° for the "true" up-wind direction of 0° have been calculated. Dash trace in Fig. 4 demonstrates retrieved azimuth NRCS curve corresponding to "measured" wind speed and up-wind direction.

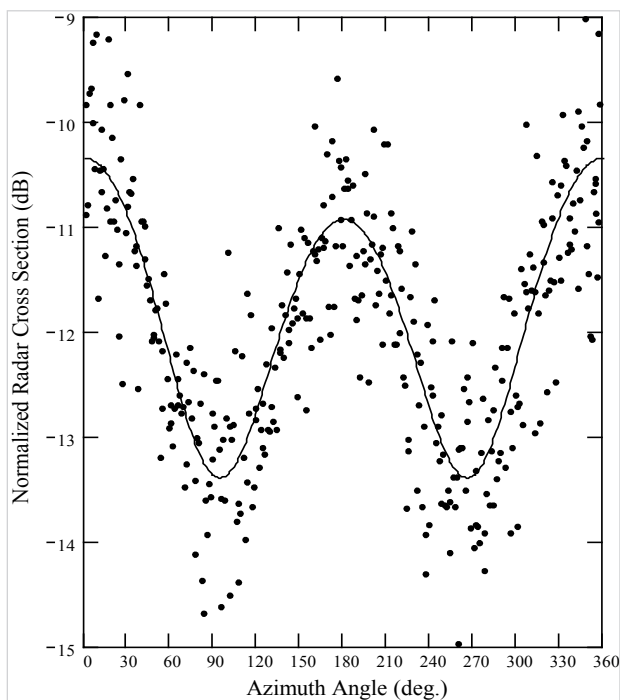


Figure 3 "Measured" NRCS after averaging of 44 samples in a one-degree azimuth sector (dot trace), and azimuth NRCS curve by model (1) at "true" wind speed of 10 m/s and "true" up-wind direction of 0° (solid trace)

Slika 3. „Izmjereni“ NRCS nakon uzimanja prosjeka iz 44 primjera u jednostupanjskom azimutnom sektoru (točkasti trag) i azimutne NRCS krivulje prema modelu (1) pri „pravoj“ brzini vjetra od 10 m/s i „pravom“ smjeru suprotnom od vjetra od 0 stupnjeva (puni trag)

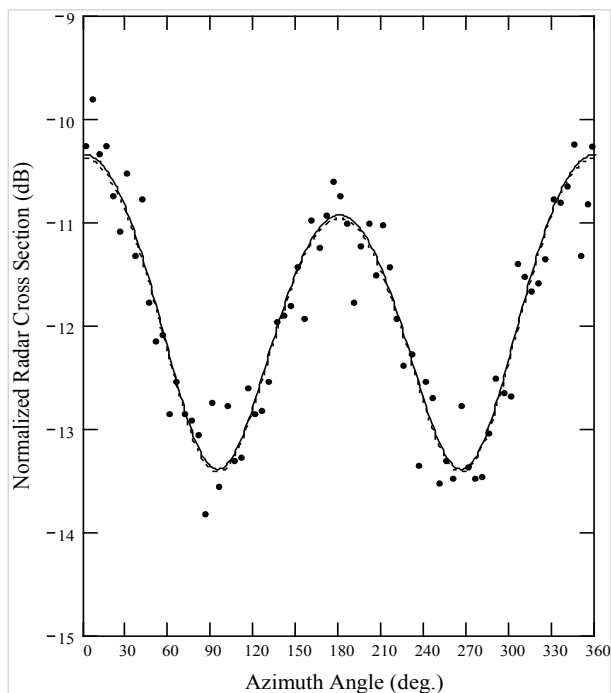


Figure 4 "Measured" NRCS after averaging of 220 samples in a five-degree azimuth sector (dot trace), azimuth NRCS curve by model (1) at the "true" wind speed of 10 m/s and "true" up-wind direction of 0° (solid trace), and azimuth NRCS curve by model (1) corresponding to "measured" wind speed of 9.95 m/s and "measured" up-wind direction of 355° (dash trace)

Slika 4. „Izmjereni“ NRCS nakon uzimanja prosjeka iz 220 primjera u petostupanjskom azimutnom sektoru (točkasti trag), azimutne NRCS krivulje prema modelu (1) pri „pravoj“ brzini vjetra od 10 m/s i „pravom“ smjeru suprotnom od vjetra od 0 stupnjeva (puni trag) te azimutne NRCS krivulje prema modelu (1) koji odgovara „izmjerenoj“ brzini vjetra od 9,95 m/s i „izmjerenom“ pravcu suprotnom od vjetra od 355 stupnjeva (trag u crticama)

Thus, this example shows us clearly the feasibility of the algorithm proposed. Other simulation results, not presented here, have shown the wind speed deviation of ± 0.2 m/s, and the direction deviation of $\pm 5^\circ$ for the wind speed range from 3 to 20 m/s, which are within the typical accuracy of the scatterometer.

5. CONCLUSION / Zaključak

The study has shown that the AWR operating in the ground-mapping mode as a scatterometer can be used for measuring the water surface backscattering signature and sea wind vector in addition to its typical navigation application.

The azimuth NRCS curve can be obtained at the circular track flight when the azimuth direction of the beam relative to the aircraft current course is fixed. The fixed beam should be pointed to the outer side of the aircraft turn to observe a greater area of sea surface and to obtain a greater number of independent NRCS samples. Azimuth position of the beam should be perpendicular to the aircraft current course, or at list tend to the perpendicular position when the scanning sector is narrower than $\pm 90^\circ$. Incidence angle of selected cell should tend to 45° that can be explained by better usage of the anisotropic properties of water surface scattering at medium incidence angles.

The proposed concept, considered principles and developed algorithm can be used for enhancement of AWR, and for designing an airborne radar system for operational measurement of the sea roughness characteristics and winds over water at joint and stand-alone observations.

Acknowledgment / Zahvala

We would like to acknowledge the financial support of this work by the Russian Science Foundation (project No. 16-19-00172). The authors would also like to express their sincere thanks to Hamburg University of Technology for the research opportunities provided. A.N. would like to thank the German Academic Exchange Service (DAAD) for an exchange visit support.

REFERENCES / Literatura

- [1] Moore, R. K.; Fung, A. K. (1979). Radar determination of winds at sea", Proceedings of the IEEE, Vol. 67, No. 11, pp. 1504-1521. <http://dx.doi.org/10.1109/PROC.1979.11510>
- [2] Melnik, Yu. A. (1980). Radar Methods of the Earth Exploration. Moscow: Sovetskoye Radio, USSR, 264 pp., in Russian.
- [3] Chelton, D. B.; McCabe, P. J. (1985). A review of satellite altimeter measurement of sea surface wind speed: With a proposed new algorithm", Journal of Geophysical Research, Vol. 90, No. C3, pp. 4707-4720. <http://dx.doi.org/10.1029/JC090iC03p04707>
- [4] Feindt, F.; Wismann, V.; Alpers, W.; Keller, W. C. (1986). Airborne measurements of the ocean radar cross section at 5.3 GHz as a function of wind speed", Radio Science, Vol. 21, No. 5, pp. 845-856. <http://dx.doi.org/10.1029/RS021i005p00845>
- [5] Masuko, H.; Okamoto, K.; Shimada, M.; Niwa, S. (1986). Measurement of microwave backscattering signatures of the ocean surface using X band and Ka band airborne scatterometers", Journal of Geophysical Research, Vol. 91, No. C11, pp. 13065-13083. <http://dx.doi.org/10.1029/JC091iC11p13065>
- [6] Wismann, V. (1989). Messung der Windgeschwindigkeit über dem Meer mit einem flugzeuggetragenen 5.3 GHz Scatterometer. Dissertation zur Erlangung des Grades eines Doktors der Naturwissenschaften. Bremen: Universität Bremen, 119 pp.
- [7] Hildebrand, P. H. (1994). Estimation of sea-surface wind using backscatter cross-section measurements from airborne research weather radar", IEEE Transactions on Geoscience and Remote Sensing, Vol. 32, No. 1, pp. 110-117. <http://dx.doi.org/10.1109/36.285194>

- [8] Carswell, J. R.; Carson, S. C.; McIntosh, R. E.; Li, F. K.; Neumann, G.; McLaughlin, D. J.; Wilkerson, J. C.; Black, P. G.; Nghiem, S. V. (1994). Airborne scatterometers: Investigating ocean backscatter under low- and high-wind conditions", *Proceedings of the IEEE*, Vol. 82, No. 12, pp. 1835-1860. <http://dx.doi.org/10.1109/5.338074>
- [9] Long, M. W. (2001). *Radar Reflectivity of Land and Sea*. New York: Artech House, USA, 534 pp.
- [10] Plant, W. J. (2003). Microwave sea return at moderate to high incidence angles", *Waves in Random Media*, Vol. 13, No. 4, pp. 339-354. <http://dx.doi.org/10.1088/0959-7174/13/4/009>
- [11] Ward, K. D.; Tough, R. J. A.; Watts, S. (2008). *Sea Clutter: Scattering, the K Distribution and Radar Performance*. London: Institution of Engineering and Technology, UK, 450 pp.
- [12] Nielsen, S. N.; Long, D. G. (2009). A wind and rain backscatter model derived from AMSR and SeaWinds data", *IEEE Transactions on Geoscience and Remote Sensing*, Vol. 47, No. 6, pp. 1595-1606. <http://dx.doi.org/10.1109/TGRS.2008.2007492>
- [13] Ouchi, K. (2000). A theory on the distribution function of backscatter radar cross section from ocean waves of individual wavelength", *IEEE Transactions on Geoscience and Remote Sensing*, Vol. 38, No. 2, pp. 811-822. <http://dx.doi.org/10.1109/36.842010>
- [14] Long, D. G.; Donelan, M. A.; Freilich, M. H.; Graber, H. C.; Masuko, H.; Pierson, W. J.; Plant, W. J.; Weissman, D.; Wentz, F. (1996). Current progress in Ku-band model functions, Technical Report MERS 96-002, Brigham Young University, USA, 88 pp.
- [15] Sosnovsky, A. A.; Khaymovich, I. A.; Lutin, E. A.; Maximov, I. B. (1990). *Aviation Radio Navigation: Handbook*. Moscow: Transport, USSR, 264 pp., in Russian.
- [16] Yanovsky, F. J. (2005). Evolution and prospects of airborne weather radar functionality and technology", *Proceedings of ICECom 2005*. Dubrovnik, Croatia, pp. 349-352. <http://dx.doi.org/10.1109/icecom.2005.204987>
- [17] Labun, J.; Soták, M.; Kurdel, P. (2012). Technical note innovative technique of using the radar altimeter for prediction of terrain collision threats", *Journal of the American Helicopter Society*, Vol. 57, No. 4, pp. 85-87. <http://dx.doi.org/10.4050/JAHS.57.045002>
- [18] Kayton, M.; Fried, W. R. (1997). *Avionics Navigation Systems*. New York: John Wiley & Sons, USA, 773 p. <http://dx.doi.org/10.1002/9780470172704>
- [19] Sosnovskiy, A. A.; Khaymovich, I. A. (1987). *Radio-Electronic Equipment of Flying Apparatuses*. Moscow: Transport, USSR, 256 pp., in Russian.
- [20] Spencer, M. W.; Graf, J. E. (1997). The NASA scatterometer (NSCAT) mission", *Backscatter*, Vol. 8, No. 4, pp. 18-24.